An Investigation on Compact Ultra-thin Triple Band Polarization Independent Metamaterial Absorber for Microwave Frequency Applications

Naveen Mishra, Dilip Kumar Choudhary, Rakesh Chowdhury, Khusboo Kumari and Raghvendra Kumar Chaudhary, *Member, IEEE*

***Abstract*— This article claims, an investigation on compact ultrathin triple band polarization independent metamaterial absorber for microwave frequency applications. The proposed absorber unit cell consist of two resonators named as Structure-A and Structure-B. Both the resonators are printed on the upper surface of dual side copper coated FR-4 epoxy glass substrate of thickness 0.8mm. The proposed absorber structure offers three distinct absorption peaks of 99.67%, 99.48% and 99.42% with FWHM bandwidth of 170 MHz (4.11-4.28 GHz), 350 MHz (9.17-9.52 GHz) and 480 MHz (11.24-11.72 GHz) at 4.19 GHz, 9.34 GHz and 11.48 GHz respectively under normal incidence. In addition to above, the four fold symmetry of proposed absorber structure make it polarization independent. Proposed absorber structure also offers more than 80% absorptivity at different angle of incidence (up to 60^0) under transvers electric and transvers magnetic polarization states. The designed absorber unit cell has compactness of 0.11 λ_0 × 0.11 λ_0 with ultra-thin thickness of 0.0111 λ_0, where λ_0 is the free space wavelength with respect to the lowest absorption peak of 4.19 GHz. Absorption mechanism of proposed unit cell has been discussed with the help of normalised input impedance, electric field distribution and surface current density plots. In order to discuss the metamaterial property of proposed absorber unit cell dispersion diagram has been shown.**

***Index Terms*— Metamaterial, Triple band Absorber, Polarization Independent, Ultra-thin.**

I. INTRODUCTION

In last decade, researchers payed their attention towards an unconventional, well-engineered designed material named Metamaterial [1]. Because of its exclusive properties of antiparallel group and phase velocities [2], this material has been widely studied in microwave engineering for antenna [3], cloaking [4], filter [5], superlens [6] and absorber [7] applications. Because of their ultra-thin, polarization independent and unity absorption properties, metamaterial emerges as a well suited substitute to fulfil the demand of modern absorber applications [7-14]. The metamaterial absorbers are configured with a periodic arrangement of compact frequency selective surfaces (FSS) on the top of the thin dielectric substrate, which is backed by copper ground plane. These absorbers are able to control their input impedance and matched it to the impedance of free space, hence unity absorptivity achieved. The absorption mechanism of these absorber structures can be understood by the electrical excitation of the top FSS structures and the magnetic excitation of substrate material. There are several single band [8-9], wide-band [10-12], and dual-band/multiband [13-17] absorber structures reported, which works on the same concept as mentioned above.

Initially metamaterial absorbers came into existence for reducing the thickness of conventional absorbers [7]. But due to their resonant approach and high quality factor, these absorbers are facing a problem of single narrow bandwidth. To solve the above mentioned problem, an orthogonally arranged scaled version of unit cell has been used [11-14]. These absorbers faces a problem of larger dimensions. Further, a single unit cell with two different resonator create the solution for this reported problem [15].

This article presents, an investigation on compact ultrathin triple band polarization independent metamaterial absorber for microwave frequency applications. The unit cell of the proposed absorber structure consists of two resonators named as Structure-A and Structure-B. Both the structures are associated with the different absorption peaks. Structure-A is responsible for the origination of single absorption peak while the two absorption peaks are associated with Structure-B. The absorption mechanism of proposed absorber has been conferred by surface current distribution and electric field density plots. The metamaterial property of proposed absorber structure has been explained with the help of dispersion diagram.

II. DESIGN AND SIMULATION RESULTS

Geometrical configuration of the proposed absorber unit cell with captions has been exhibit in Fig. 1. It consist of two resonators entitled as Structure-A and Structure-B. Structure-A is designed with two concentric rings connected by four distinct strips. Further, the outer ring splits diagonally into four equal parts. Similarly, Structure-B is the scaled version of Structure-A with a change of the outer split rectangular ring. Both the resonators are printed on the upper layer of the double sided copper ($\sigma = 5.8 \times 10^7$ S/m) coated FR-4 epoxy glass substrate ($\varepsilon_r = 4.4$, $tan\delta = 0.02$) of thickness 0.8mm and are responsible for the distinct absorption peaks. The bottom layer of the proposed absorber structure offers complete

The authors are with the Department of Electronics Engineering, Indian Institute of Technology (Indian School of Mines), Dhanbad, 826004, India (e-mail: naveenmishra.ece@gmail.com; dilip.choudhary6@gmail.com; rc4076@gmail.com; khusbookumari.ece@gmail.com; raghvendra.chaudhary@gmail.com).

copper backing with a copper thickness of 35µm which is greater than the skin depth of copper at all the absorption frequencies Eqn. (1) [18], and restrict the further propagation of the incident wave.

$$\delta = \sqrt{\frac{\rho}{\pi f \mu}} \qquad (1)$$

where δ represents skin depth, ρ is resistivity associated with the conductor in $\Omega.m$, μ is permeability of conductor in H/m and f is the frequency in Hz. In order to analyse the absorptivity of the designed absorber structure, proposed unit cell is applied with the master-slave periodic boundary conditions of HFSS 14.0 3-D electromagnetic simulation software. Mathematically, absorption coefficient for any structure can be calculated by Eqn. (2).

$$A = \left(1 - \left|S_{11}\right|^2 - \left|S_{21}\right|^2\right) \qquad (2)$$

Since the proposed absorber structure is designed with the complete copper ground plane which restrict the incidence wave propagation and results into zero transmission. So Eqn. (2) can be rearrange in the form of Eqn. (3).

$$A = \left(1 - \left|S_{11}\right|^2\right) \qquad (3)$$

where $\left|S_{11}\right|^2$ represent reflected power and $\left|S_{21}\right|^2$ is transmitted power.

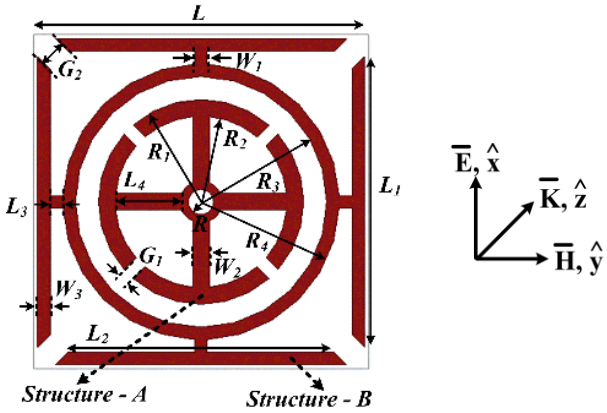

Fig.1 Geometrical configuration of the proposed absorber unit cell. [All dimensions are in mm: $L = 8$, $L_1 = 6.95$, $L_2 = 6.35$, $L_3 = 0.3$, $L_4 = 1.58$, $G_1 = 0.3$, $G_2 = 0.6$, $R = 0.3$, $R_1 = 2.45$, $R_2 = 2.05$, $R_3 = 3$, $R_4 = 3.3$, $W_1 = 0.3$, $W_2 = 0.4$, $W_3 = 0.3$.]

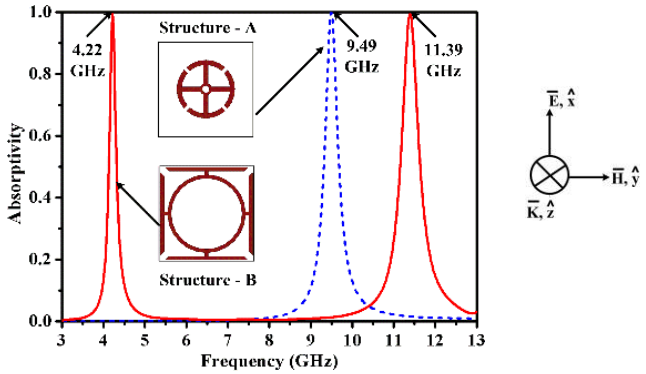

Fig. 2. Absorptivity curve for both the individual structures.

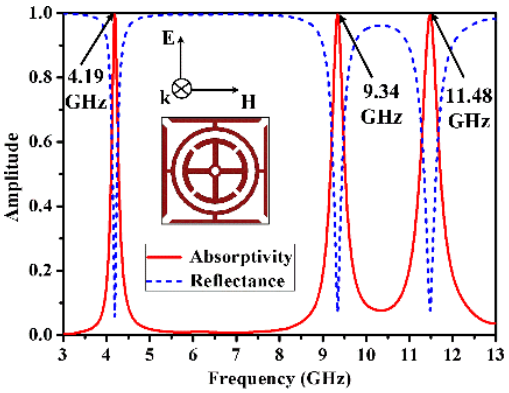

Fig. 3. Absorptivity and reflectance curve for the proposed absorber structure under normal incidence.

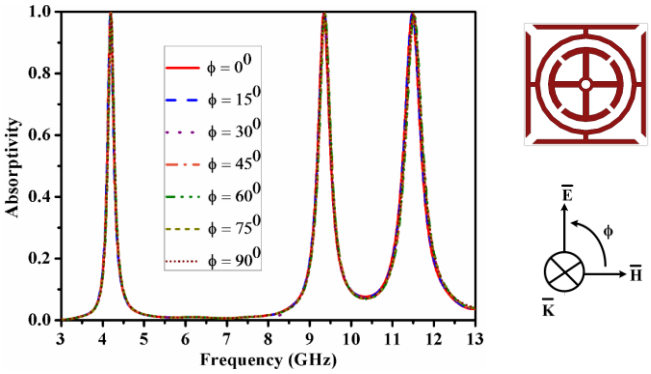

Fig. 4. Absorptivity curve of proposed absorber structure at different polarization angles.

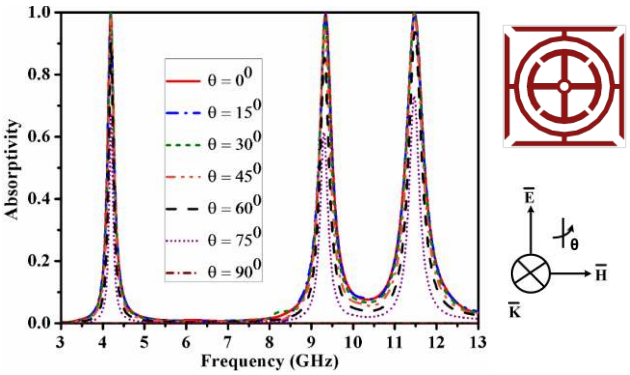

Fig. 5 (a). Absorptivity curve of proposed absorber structure at different incidence angles under TE polarization.

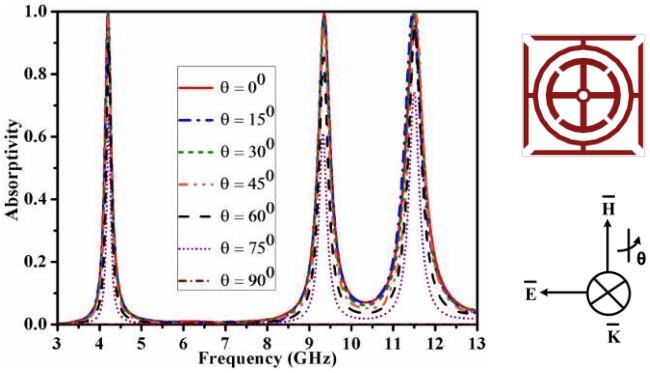

Fig. 5 (b). Absorptivity curve of the proposed metamaterial absorber at different incidence angles under TM polarization.

Fig. 2 shows the absorptivity curve for Structure-A and Structure-B separately. On the basis of observations it can be conclude that the origination of first (99.41% at 4.22 GHz) and third (99.39% at 11.39 GHz) absorption peaks are associated with Structure-B while the second (99.97% at 9.49 GHz) absorption peak is due to Structure-A. Further, both the structures are combined to design proposed metamaterial absorber unit cell. Absorptivity and reflectance plots along with the direction of field vectors (wave propagation, electric field and magnetic field vectors) for the designed absorber structure has been depicted in Fig. 3. After combining both the structures, a negligible amount of shift in all the three absorption peaks are observed. This shift in absorption frequencies is due to the coupling between Structure-A and Structure-B. In addition to above, at all the three absorption peaks near unity absorption and close to zero reflection coefficient achieved. Proposed absorber structure exhibits three distinct absorption band with peak absorptivity of 99.67%, 99.48% and 99.42% at 4.19 GHz, 9.34 GHz and 11.48 GHz respectively under normal incidence. The full width at half maximum (FWHM) bandwidth around all three absorption peaks are 170 MHz (4.11-4.28 GHz), 350 MHz (9.17-9.52 GHz) and 480 MHz (11.24-11.72 GHz) respectively.

Fig. 4 exhibits the simulated absorptivity curve of the proposed absorber structure under normal incidence of electromagnetic waves for different polarization angles. During the study of absorptivity at different polarization angles, the direction of propagation of electromagnetic wave remains fix while the direction of E and H fields are rotating at different ϕ values. It can be observed that the proposed absorber structure shows almost similar absorption at different polarization angles (ϕ = 0^0 to 90^0 at a step of 15^0), hence polarization independent. The polarization independent characteristics of the designed absorber structure can be explained by the four fold rotational symmetry of the unit cell. Further, the absorption behaviour of designed absorber structure under transvers electric (TE) and transvers magnetic (TM) polarization states has been demonstrated in Fig. 5(a) and Fig. 5(b) respectively. In the study of absorption behaviour of designed absorber structure under TE polarization state, the direction of propagation of electromagnetic wave as well as the direction of magnetic field rotates at different incidence angles (θ) while the electric field direction remains unchanged. Similarly in case of TM polarization direction of propagation of electric field and incident electromagnetic wave rotates at different incidence angles while the direction of magnetic field remains unchanged. It can be observed that for both the polarization states (TE and TM) the designed absorber structure offers more than 80% absorptivity up to 60^0 of incidence angles.

A. *Discussion of MTM Property for the Proposed Absorber Structure:*

In order to discuss the metamaterial behaviour of the designed absorber structure dispersion curve has been calculated by Eqn. (4) and depicted in Fig. 6. The dispersion graph is divided in two major sections one is right-handed (RH) region where the slope of the dispersion curve is positive i.e. group and phase velocities are in parallel, while the other one is left-handed (LH) region where slope of the curve is negative i.e. phase and group velocities are anti parallel. It can be observed that all three absorption bands ((4.11-4.28 GHz), (9.17-9.52 GHz) and (11.24-11.72 GHz)) lies in the left handed regions ((3-4.54 GHz), (7.14-9.58 GHz) and (10.41-12.29 GHz)) respectively.

$$\beta d = \cos^{-1}\left(\frac{1 - S_{11}S_{22} + S_{12}S_{21}}{2S_{21}}\right) \qquad (4)$$

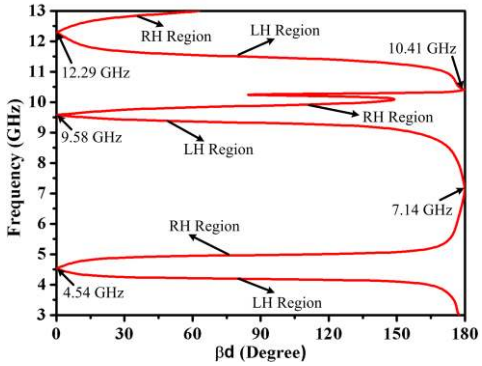

Fig. 6. Dispersion diagram for the designed absorber unit cell.

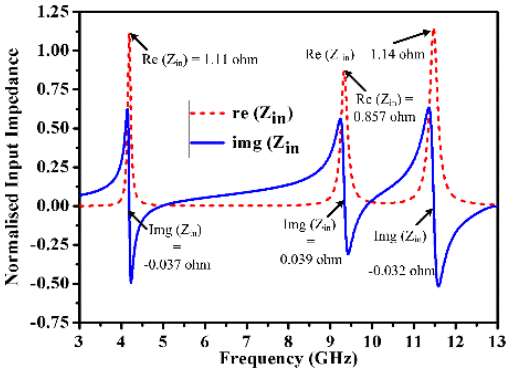

Fig. 7. Normalised input impedance plot for the proposed ultra-thin metamaterial absorber.

B. *Absorption Mechanism of Proposed MTM Absorber Structure:*

The absorption mechanism of the proposed absorber structure can be understood with the help of normalised input impedance, electric field distribution and surface current density plots under normal incidence. Normalised input impedance of the proposed absorber structure has been shown in Fig.7. It is clearly seen that at all the absorption peaks the real value of normalised input impedance is near to unity while the imaginary part is near to zero. Since the input impedance at all the three absorption peaks are nearly equal to the free space impedance (377 + *j*0), so a less amount of reflection occurs and near unity absorption achieved. Input impedance of the proposed absorber structure can be mathematically expressed by Eqn. (5).

$$Z_{in} = \sqrt{\frac{(1+S_{11})^2 - (S_{21})^2}{(1-S_{11})^2 - (S_{21})^2}} \qquad (5)$$

This article has been accepted for publication in a future issue of this journal, but has not been fully edited. Content may change prior to final publication. Citation information: DOI 10.1109/ACCESS.2017.2675439, IEEE Access

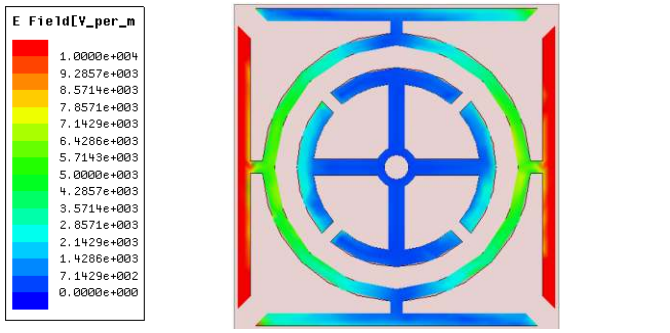

(a) 4.19 GHz

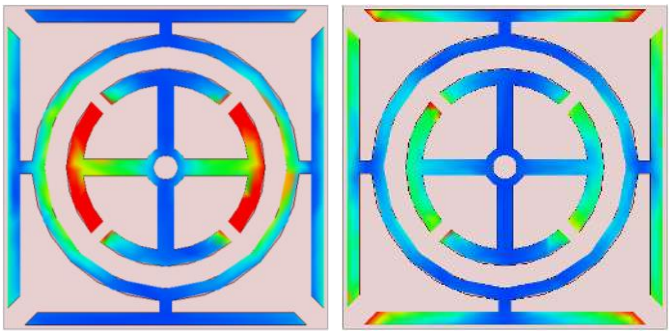

(b) 9.34 GHz (c) 11.48 GHz

Fig. 8. Electric field distribution on the proposed absorber structure at all the absorption peaks.

Fig. 8 depicts the electric field concentration plot for all three absorption peaks (Fig. 8 (a) at 4.19 GHz, Fig. 8 (b) at 9.34 GHz and Fig. 8 (c) at 11.48 GHz). The surface current distribution plot on both the copper layers (upper and lower) at 4.18 GHz, 9.34 GHz and 11.48 GHz are shown in Fig. 9 (a), Fig. 9 (b) and Fig. 9 (c) respectively. It can be observed that at the frequencies of 4.19 and 11.48 GHz the maximum concentration of electric field and surface current distribution has been achieved on the Structure-B, while at the absorption peak of 9.34 GHz maximum concentration is on Structure-A. It can also observed from all the surface current distribution plots that the direction of flow of surface current in upper and lower copper layers are opposite and forms a circulating current which is responsible for the magnetic excitation while the electric field concentration on the upper layer (Structure-A and Structure-B) of the proposed absorber structure is responsible for the electric excitation. In order to achieve the maximum absorption electric and magnetic excitations should occur simultaneously.

In case of TE polarization under different incidence angles electric field remains fixed while the concentration of surface circulating current reduces and due to the reduction of surface circulating current magnetic excitation reduces, hence absorptivity degraded. Similarly, In case of TM polarization concentration of surface circulating current remains unchanged while the electric field density degraded with the increase in incidence angle. It degrade the electric excitation and results in reduction of absorptivity.

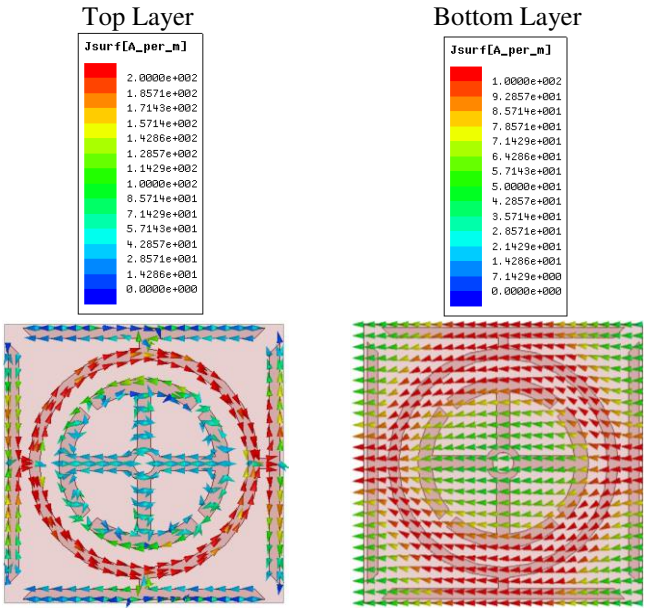

(a) at 4.19 GHz

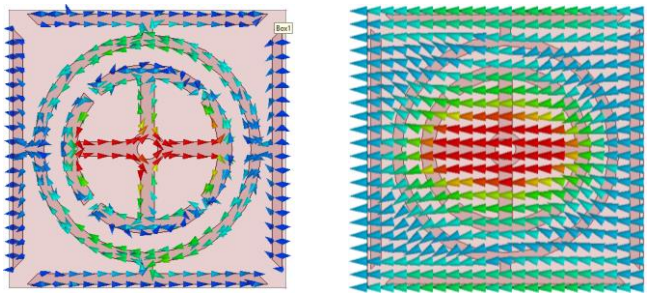

(b) at 9.34 GHz

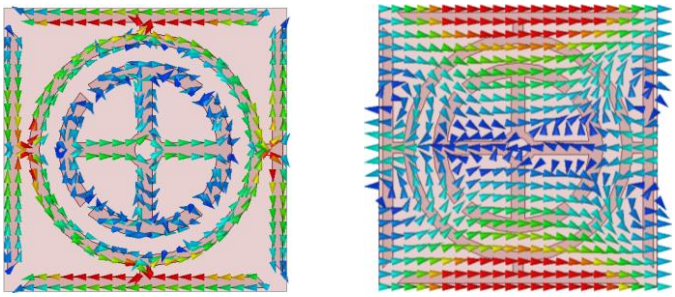

(c) at 11.48 GHz

Fig. 9. Surface current distribution on the proposed absorber structure at all the absorption peaks.

III. Effect of Various Parameters on Absorption Coefficient

A. *Bandwidth Improvement:*

Fig. 10 depicts the variation in absorptivity curve by varying the length L_1. It can be observed that as the length L_1 increases from 4mm to 4.6mm, the radius of split ring increases (keeping the split ring thickness (R_1-R_2) unchanged), the second absorption peak starts shifting towards the lower

frequencies while the other two absorption peaks remains unchanged. This shift in second absorption peak is due to the increment of inductance associated with the area of the split ring of structure-A. In order to improve the bandwidth of the proposed absorber structure L_1 is optimised to 4mm where the second absorption peak merged with the third absorption peaks and enhanced FWHM bandwidth of 1.07 GHz (10.58-11.65 GHz) is achieved.

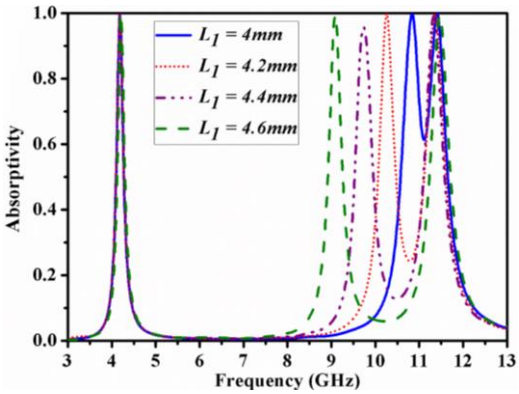

Fig. 10. Simulated absorptivity curve by varying L_1.

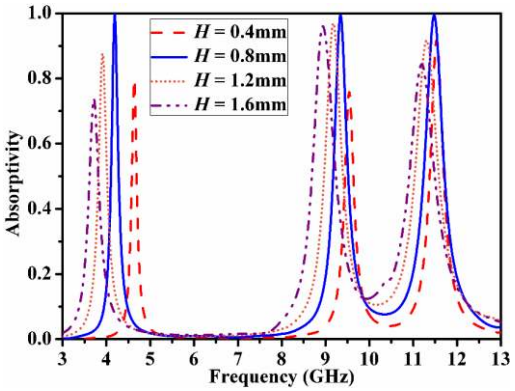

Fig. 11. Simulated Absorptivity curve at different values of substrate thickness (H).

B. *Variation of Substrate Thickness:*

Effect on absorptivity with the variation of substrate thickness (H) is shown in Fig. 11. By increasing substrate thickness from 0.4 mm to 1.6 mm, all the absorption peaks starts shifting towards lower frequencies. The increment in substrate thickness corresponds to decrement in capacitance between the upper and lower copper layers and also responsible for the increment in the inductance associated with the upper copper layer [19]. This reduction in capacitance and increment in inductance is responsible for the shift in all three absorption peaks towards lower frequency.

IV. Experimental Results

Fig. 12 depicts the experimentally developed fabricated proto-type for the 37×37 array of the proposed absorber structure printed on the 0.8mm thick FR-4 epoxy glass substrate. Block-diagram for the measurement setup of absorber has been shown in Fig. 13, which requires a similar pair of horn antennas (working in the complete absorption bands), fabricated proto-type, sample holder and vectored network analyzer. In this measurement process a pairs of horn antennas, each for C- and X- band separately with Agilent N5221A PNA vectored network analyzer has been used. Because of the non-availability of anechoic chamber the complete measurement has been carried out in free space.

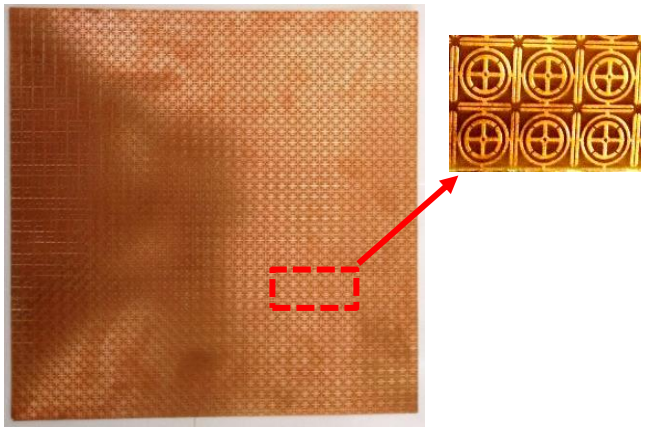

Fig. 12. Experimentally developed proto-type of proposed absorber structure.

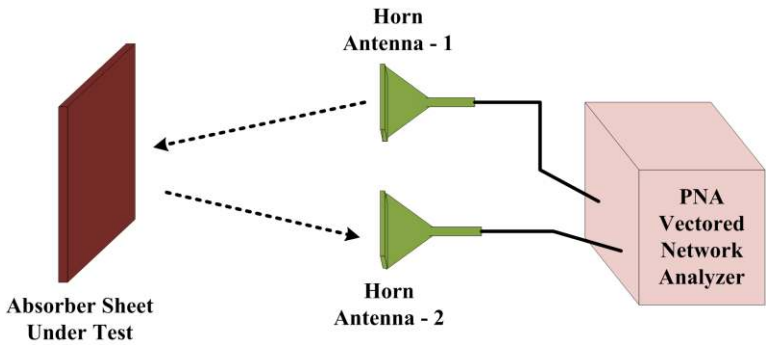

Fig. 13. Block-diagram for the measurement setup of absorber.

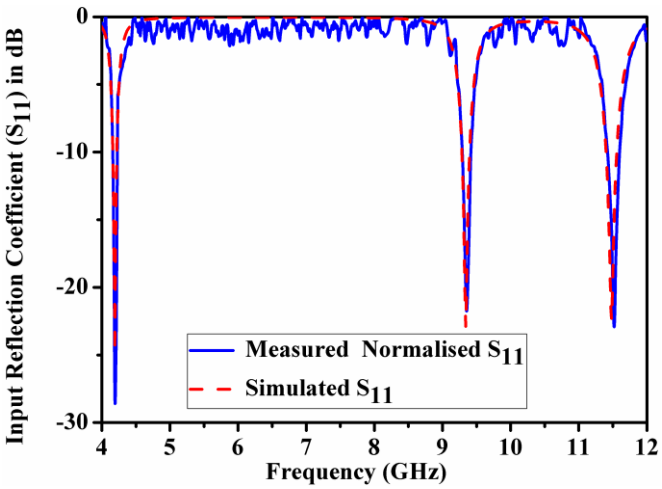

Fig. 14(a). Simulated and measured input reflection coefficient curve for the proposed absorber structure.

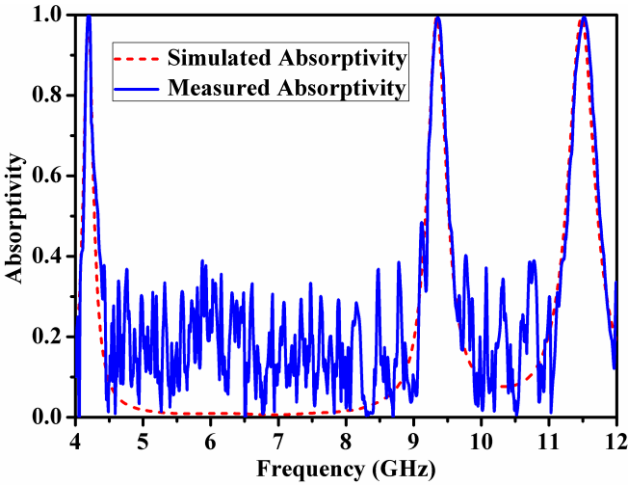

Fig. 14(b). Simulated and measured absorptivity curve for the proposed absorber structure.

Initially, the input reflection coefficient for the plane copper sheet has been measured as a reference. Further, the fabricated proto-type has been placed at the same distance and input reflection coefficient for the designed absorber proto-type has been measured. Now the measured input reflection coefficient for the designed absorber structure has been normalised with the measured reference. The absorption coefficient can be calculated with the help of normalised input reflection coefficient as mentioned in Eqn. (3). Fig. 14(a) and Fig. 14(b) depicts the simulated and measured normalised input reflection coefficient and absorptivity curve for the fabricated proto-type. Experimentally developed prototype of the proposed absorber structure offers three absorption peaks at 4.20, 9.36 and 11.53 GHz with peak absorption value of 99.97%, 99.43% and 99.45% respectively. Simulated and measured results shows good agreement with each other except ripples in non-absorption bands. Since the measurement environment is free space so this may be the cause for the origination of ripples in outside of the absorption bands. Table I shows the comparison chart for different parameters of proposed absorber structure with the previously published metamaterial absorber structures.

Table I - Comparison of the proposed work with the earlier published MTM absorber structures.

Parameters	UCS* (mm^3)	UCS* corresponds to LF* (λ_0)	No. of absorption band	LAP* (GHz)
This work	8 × 8 × 0.8	0.11 × 0.11 × 0.011	Triple	4.19
[13]	15 × 15 × 1	0.37 × 0.37 × 0.024	Triple	7.46
[14]	18 × 18 × 1	0.31 × 0.31 × 0.017	Triple	5.22
[17]	11 × 11 × 1	0.12 × 0.12 × 0.011	Triple	3.25

*UCS – Unit Cell Size; LF – Lowest Frequency; LAP – Lowest Absorption peak

V. CONCLUSION

This article presents an investigation on compact ultra-thin triple band polarization independent metamaterial absorber for microwave frequency applications. Proposed absorber structure offers three absorption bands with near unity absorption peak value. In order to understand the absorption mechanism of proposed absorber structure normalised input impedance, electric field distribution and surface current density plots has been discussed. The proposed absorber structure shows compactness of 0.11 λ_0 × 0.11 λ_0 with ultra-thin thickness of 0.0111 λ_0, where λ_0 is the free space wavelength with respect to the lowest absorption peak of 4.19 GHz. The metamaterial characteristics of the proposed absorber structure has been explained with the help of dispersion diagram. The designed absorber structure can be used for various wireless communication and defense applications.

REFERENCES

[1] C. Caloz and T. Itoh, "Electromagnetic Metamaterials: Transmission Line Approach and Microwave Applications," John Wiley and Sons, 2005.

[2] V.G. Veselago, "The Electrodynamics of substances with simultaneously negative values of ε and μ," Soviet Physics Uspekh Usp. Fiz. Nauk 92, pp. 509 – 514, July, 1964.

[3] N. Mishra, R. K. Chaudhary, "A miniaturized ZOR antenna with enhanced bandwidth for WiMAX applications," Microwave and Optical Technology Lett., vol. 58, pp. 71-75, 2016.

[4] D. Schurig, J.J. Mock, B.J. Justice , S.A. Cummer, J.B. Pendry, A.F. Starr, and D.R. Smith, "Metamaterial electromagnetic cloak at microwave frequencies," Science 314, pp. 977 – 980, 2006.

[5] J. Kim, C.S. Cho and J.W. Lee, "CPW bandstop filter using slot type SRRs," Electronics Lett., vol. 41, 2005.

[6] N. Fang, H. Lee, C. Sun , and X. Zhang, "Sub – diffraction – limited optical imaging with a silver super lens," Science 308, pp. 534 – 537 2005.

[7] F. Bilotti, L. Nucci, L. Vegni, "An SRR based microwave absorber," Microwave and Optical Technology Lett., vol. 48, pp. 2171-2175, 2006.

[8] S. R. Thummaluru, N. Mishra, and R. K. Chaudhary, "Design and analysis of an ultra-thin X-band polarization – insensitive metamaterial absorber," Microwave Optical Technology Lett. Vol.58, No. 10, pp. 2481-2485, October 2016.

[9] B. Wang, T. Koschny and C. M. Soukoulis, 'Wide-angle and polarization-independent chiral metamaterial absorber', Phys. Rev. B, 2009, 80, pp. 033108.

[10] J. Lee and S. Lim, "Bandwidth enhanced and polarization-insensitive metamaterial absorber using double resonance," Electronics Lett., vol. 47, 2011.

[11] S. Ghosh, S. Bhattacharyya and K. V. Srivastava, "Bandwidth-enhancement of an ultrathin polarization insensitive metamaterial absorber," Microwave and Optical Technology Lett., vol. 56, pp. 350-355, 2014.

[12] M. R. Soheilifar and R. A. Sadeghzadeh, "Design, simulation, and fabrication of an ultrathin planar microwave metamaterial absorber," Microwave and Optical Technology Lett., vol. 56, pp. 2916-2922, 2014.

[13] Hui Li, Li Hua Yuan, Bin Zhou, Xiao Peng Shen, Qiang Cheng, and Tie Jun Cui, "Ultrathin multiband gigahertz metamaterial absorbers," Journal of Applied Physics, 110, 014909, 2011.

[14] S. Bhattacharyya, S. Ghosh and K. V. Srivastava, "Triple band polarization-independent metamaterial absorber with bandwidth enhancement at X-band," Journal of Applied Physics, 114, pp. 094514, 2013.

[15] D. Chaurasiya, S. Ghosh and K. V. Srivastava, "Dual band polarization-insensitive wide angle metamaterial absorber for radar application," 44th European Microwave Conf., Rome, Italy, pp. 885–888, 2014.

[16] H. Zhai, Z. Li, L. Li and C. Liang, "A dual-band wide-angle polarization-insensitive ultrathin gigahertz metamaterial absorber," Microwave and Optical Technology Lett. vol. 55, pp. 1606-1609, 2013.

[17] H. Zhai, C. Zhan, Z. Li, and C. Liang, "A triple-band ultrathin metamaterial absorber with wide angle and polarization stability," IEEE Antenna and Wireless Propa. Lett., vol. 14, pp. 241-244, 2015

[18] D. M. Pozar, "Microwave Engineering," second edition, John Wiley and Sons, 2005.

[19] F. Costa, A. Monorchio, and G. Manara, "An equivalent-circuit modeling of high impedance surfaces employing arbitrarily shaped FSS," in Proc. ICEEA, Turin, Italy, pp. 852–855, 2009.